

## X-ray tube with needle-like anode

Mieczysław Słapa,  
Włodzimierz Straś,  
Marek Traczyk,  
Jerzy Dora,  
Mirosław Snopek,  
Ryszard Gutowski,  
Wojciech Drabik

**Abstract** An X-ray tube with a needle-like anode (NAXT) built in our Laboratory, its design and basic operating parameters are presented. The process of electron beam forming and influence of external and internal magnetic fields is discussed. The tube properties essential from the point of view of its application in X-ray generators as well as disadvantageous thermal effects caused by flow of heat generated in the tube target to irradiated objects are discussed. The tube is almost a point-like source of X radiation emitted into  $4\pi$  geometry; the dose rates are on the order of 1 Gy/min at the distance of 10 mm from the anode cap. Preliminary tests show the tube may be useful in brachytherapy of cancer tumors of diameter up to 30 mm. The tube may also be an interesting device in widely understood field of irradiation techniques.

**Key words** brachytherapy • photon needle • X-ray tube

### Introduction

The project to build an X-ray tube with a needle-like anode may be traced back to the idea of application of X-rays to brachytherapy [5]. In the classical brachytherapy an isotope source is placed inside the tumor in order to destroy (by means of radiation) the cancer tissue, preserving the more distant normal tissues. If an X-ray generator is to be used instead of the isotope source, the point where the electron-photon conversion takes place and the X-rays are actually generated – i.e. the tube target – must be introduced inside the tumor. This requirement calls for a long and thin tube anode, which may be described as “needle-like”; the tube target is placed at the end of this anode.

The needle-like anode in the NAXT tube is a result of developing classical drift chamber of an X-ray tube into a long, thin pipe [1]. Drift chamber is the anode region, in which there is no electric field. Drift chambers are commonly used in X-ray tubes since they enable to reduce radiation doses absorbed in the tube insulators, and to improve the tube's cooling [4]. In order to increase length of the drift chamber to several centimeters, one has to precisely form and focus the electron beam traveling to the tube target, and effectively shield it from external and internal magnetic fields.

Basic advantage of the NAXT tube is the capability to deliver radiation doses to well defined objects without irradiating their surroundings, and maximum utilization of X-rays generated in the electron-photon conversion process.

NAXT two main disadvantages are: (i) susceptibility of electron beam traveling to the tube target to external and internal magnetic fields, and (ii) part of heat generated in the tube target has to be dissipated within the irradiated object.

M. Słapa, W. Straś, M. Traczyk<sup>✉</sup>, M. Snopek, W. Drabik  
The Andrzej Sołtan Institute for Nuclear Studies,  
05-400 Otwock-Swierk, Poland,  
Tel.: +48 22/ 718 05 61, Fax: +48 22/ 779 34 81,  
e-mail: marekt@ipj.gov.pl

J. Dora  
Power Dora System,  
110 S. Wyszynskiego Str., 50-307 Wrocław, Poland

R. Gutowski  
Uniquant  
14/9 Batalionu Parasol Str., 01-118 Warsaw, Poland

Received: 8 August 2001, Accepted: 22 February 2002

New design of the NAXT tube developed in our Lab employs a cylindrical acceleration chamber instead of the so-far used flat, parallel chambers. The new chamber improves the electron beam symmetry and is easier to manufacture. The design was developed with brachytherapy application in mind, where the tube anode must be introduced inside brain through a biopsy hole of only 3 mm in diameter. The developed tube is a component of the "Photon Needle" X-ray generator under development in our Institute.

### Design of the X-ray tube with needle-like anode

Design of the NAXT tube developed in our Lab is shown in Fig. 1. Conceptually it is a two-stage device. Intensity of the electron beam and its space position is determined in the first stage, the second stage accelerates the beam to the required energy and transports it to the tube target. The first stage is made of the selected fragment of electron gun from the Vela 2 kinescope. The second stage consists of a cylindrical acceleration chamber coupled with a long drift chamber. The drift chamber is made of the so-called  $\mu$ -metal tube; the tube length is 180 mm, diameter is 3 mm, and wall thickness is 0.5 mm. The beryllium cap at the end of the drift chamber serves as the exit window for X-rays. At the very end and inside the cap a 1.0 mg/cm<sup>2</sup> layer of gold forms the tube target.

Electrons emitted from indirectly heated oxide cathode are formed by the  $S_2$  grid into a beam with angle divergence below 1 degree. The  $S_1$  grid voltage controls the beam intensity. Electrons initially accelerated by the intermediate anode accelerate further within the cylindrical acceleration chamber to  $eU_a$  energy (where  $U_a$  is the anode voltage), and finally are injected into the region without electric field i.e. into the drift chamber. Within the drift chamber they continue to move along trajectories established during acceleration process. Correct acceleration process guarantees that all the injected electrons finally arrive to the target.

The process of forming electrons in a beam may in the NAXT tube be regarded as subsequent focusing by two electrostatic lenses: the first one being the Vela 2 electron gun acceleration chamber, and the second one – the NAXT acceleration chamber. The design of the latter was based on the results of mathematical modeling. Electron trajectories for the given set of lenses were calculated vs. parameters of the latter chamber (various electrode spacing, and diameters of the electrode cylinders) and vs.  $U_p/U_a$  ratio of the accelerating voltages (where  $U_p$  is of the intermediate anode voltages, and  $U_a$  is the anode voltage). Examples of

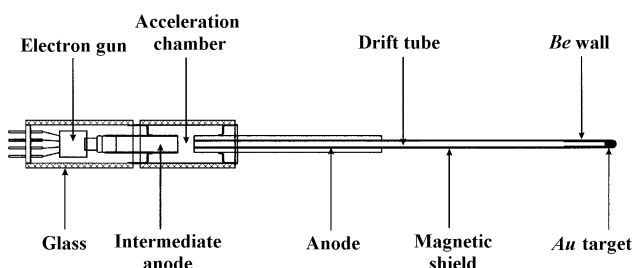


Fig. 1. Design of the X-ray tube with needle-like anode.

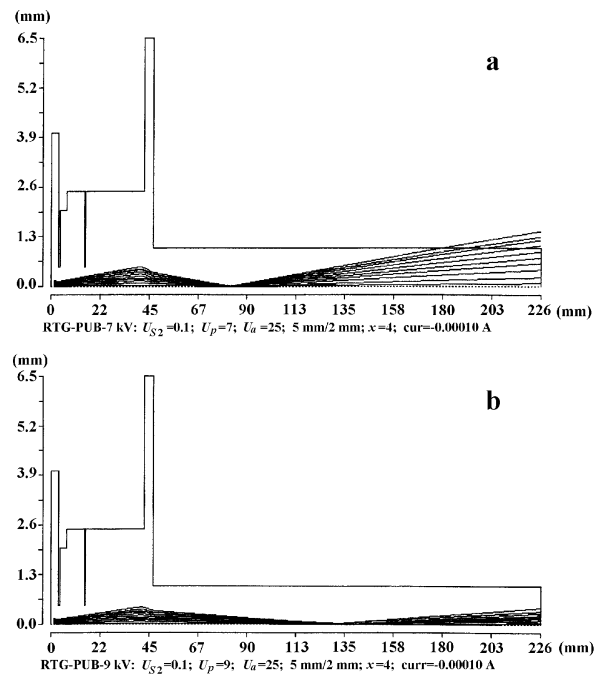


Fig. 2. Electron trajectories for  $U_p/U_a$  equal to: a – 7 kV/25 kV; b – 9 kV/25 kV.

the trajectories shown in Fig. 2 have been calculated assuming  $U_p/U_a = 7$  kV/25 kV and  $U_p/U_a = 9$  kV/25 kV, at the following chamber parameters: electrode spacing  $x = 4$  mm, electrode diameters 5 mm and 2 mm, and the grid voltage  $U_{S2} = 0.1$  V.

The calculations show that electron beam spot size at the tube target depends on both the  $U_p/U_a$  ratio, and the design parameters of the NAXT acceleration chamber.

The measured focal spot size of the electron beam at the tube target vs.  $U_p$  for constant  $U_a = 25$  keV is shown in Fig. 3. The spot photographs taken for three selected  $U_p$  values are shown in Fig. 4.

### Influence of magnetic fields on the electron beam

In classical X-ray tubes, the target-to-cathode distance is practically the same as the anode-to-cathode distance (a fraction of one centimeter to a few centimeters). On the other

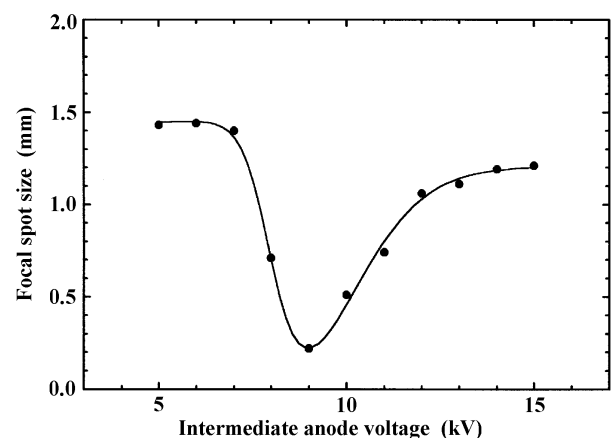


Fig. 3. Measured focal spot size of the electron beam at the tube target vs. intermediate anode voltage  $U_p$ .

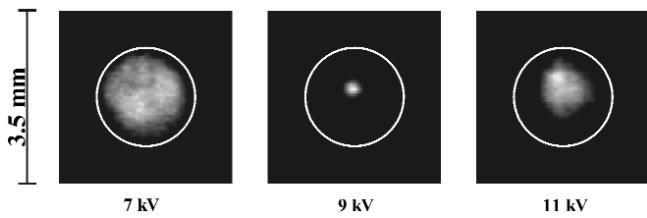


Fig. 4. Pictures of spots of the electron beam at the tube target for three selected  $U_p$  values.

hand, the cathode-to-target distance in the NAXT tubes is much larger than the acceleration track, and electron trajectories are significantly longer than those in classical tubes – they may reach 20 centimeters.

Magnetic field affects moving electrons with the Lorentz force:

$$(1) \quad \vec{F} = e\vec{v} \times \vec{B}$$

where:  $e$  – electron charge;  $\vec{v}$  – electron velocity;  $\vec{B}$  – magnetic induction.

The Lorentz force does not change energy of the electrons, but may influence their trajectories and in consequence may decline the beam from the target to some point on the drift chamber wall. Shift of an electron beam caused by a constant magnetic field  $B$  may be expressed as:

$$(2) \quad s = \frac{eB_p l^2}{2m v} = \frac{B_p l^2}{2} \sqrt{\frac{e}{2U_a m}}$$

where:  $B_p$  – component of the magnetic induction vector perpendicular to the direction of the electron movement,  $l$  – length of the drift chamber,  $U_a$  – anode voltage,  $m$  – electron mass.

Magnetic field within a tube is generally a vector sum of the Earth magnetic field, other external magnetic fields, and internal fields generated by constructional elements of the tube. Influence of each of these sources must be minimized in order to preserve trajectories defined by the electrostatic optics in the NAXT tube, at least to prevent shifting the electron beam outside the target.

Influence of internal fields is minimized by selection of diamagnetic and paramagnetic materials for constructional elements of the tube, and by careful optimization of shapes

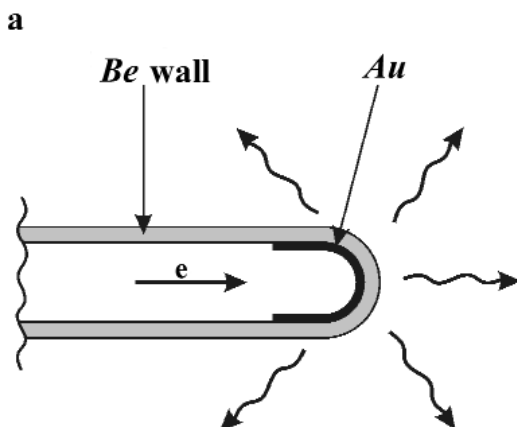


Fig. 6. a – Layout of the NAXT target and radiation exit window; b – Photograph of the working target.

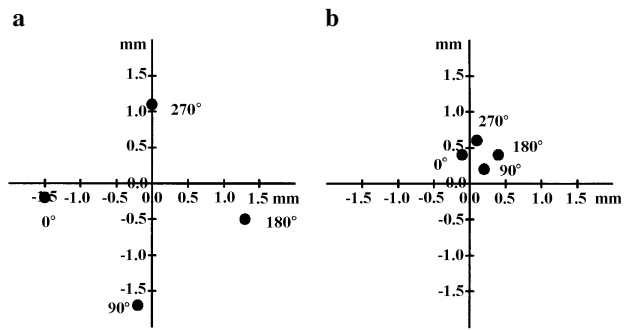


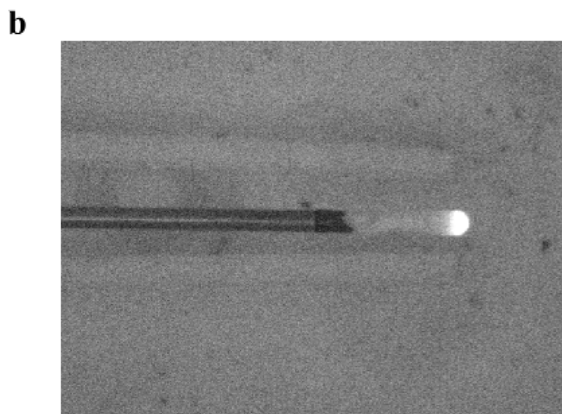
Fig. 5. Focal spot localization vs. orientation of the drift chamber in relation to the Earth magnetic field (dependence on angle of rotation around the drift chamber symmetry axis). a – without  $\mu$ -metal shielding; b – with  $\mu$ -metal shielding.

and dimensions of elements made of materials containing Fe or Ni, as well as by special technological processing of these materials.

Influence of external fields (including the Earth magnetic field) is minimized by use of the so-called magnetic shields. The commonly used for such shields  $\mu$ -metal is a material with magnetic permeability greater than 100,000; it may be used alone, or in combination with a ferromagnetic of magnetic permeability on the order of several units. In any given tube magnetic field may vary from point to point. Final shift of the electron beam will be given by superposition of partial shifts on subsequent segments of the beam trajectory.

A test tube with 5 mm internal diameter of drift chamber made of stainless steel has been manufactured to study influence of the Earth magnetic field on the electron beam trajectories in NAXT tubes. After the beam has been optimally focused on the target, the focal spot localization was observed vs. orientation of the drift chamber in relation to the Earth magnetic field. The dependence on angle of rotation around the drift chamber symmetry axis is shown in Fig. 5a. Maximum shift caused by the Earth magnetic field amounted to 2.8 mm. This means that the beam would not successfully reach the target if the drift chamber had only 2 mm internal diameter (which is the value we aim at).

Similar measurements have been made for a NAXT tube with a 2 mm internal diameter drift chamber made of  $\mu$ -metal; results are illustrated in Fig. 5b. Further improvement would require placing magnetic shielding also between the electron gun and the intermediate anode.



## NAXT tube as an X-ray generator

The NAXT tube is designed as an isotropic source of X radiation generated with a possibly high efficiency in the electron-photon conversion process, and emitted into  $4\pi$  geometry. These conditions determine design of the tube target and the radiation exit window as shown in Fig. 6a. Target is made of homogeneous layer of gold deposited on the inside wall of a beryllium cap. Thickness of the layer ( $1 \text{ mg/cm}^2$ ) is determined by the range of 30 keV electrons in gold, whereas its length (4 mm) must be enough to allow conversion of back-scattered electrons into photons. Photograph of the working tube target is shown in Fig. 6b; the cap in this tube has been covered with a luminophore to the length of 20 mm.

In such geometry it is difficult to calculate theoretical relation between the electron beam parameters and parameters of the generated X-ray beam. The calculations based on the Monte Carlo techniques are in progress. However, the X beam intensity  $I_x$  and yield  $\eta$  of radiation generation may be estimated for continuous part of the radiation spectrum (assuming that the target thickness is comparable with the range of electrons) [2]:

$$(3) \quad I_x = \sum n_i E_i = 1.3 \times 10^{-9} Z U_a^2 I_a$$

$$(4) \quad \eta = 1.3 \times 10^{-9} Z U_a$$

where  $n_i$  is the number of photons with energy  $E_i$ ,  $Z$  is the target atomic number, and  $I_a$  is the anode current. Taking  $U_a = 30 \text{ kV}$  and the mean photon energy as  $0.5 eU_a$  one can calculate that the current  $1 \mu\text{A}$  will generate  $3.8 \times 10^{10}$  photons/s, which is approximately equivalent to 1 Ci.

Characteristic L lines of Au are significant components of the X-ray spectrum generated in NAXT tubes. The lines come from direct ionization of L shells in gold atoms by decelerated electrons, and from secondary fluorescence by brehmstrahlung radiation; they significantly modify the mean radiation energy determining interaction with tissues.

An example of X radiation spectrum generated in the NAXT tube working at  $U_a = 30 \text{ kV}$ ,  $I_a = 1 \mu\text{A}$  and taken during 300 s with the help of a HPGc detector is shown in Fig. 7. The detector was placed 70 cm away from the anode and equipped with an aperture of 2 mm diameter. Number of

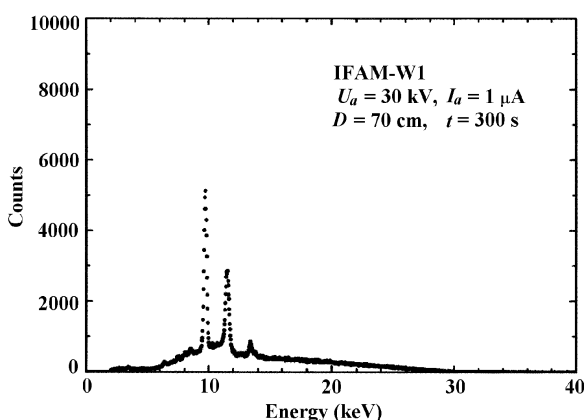


Fig. 7. Spectrum of X radiation from the NAXT tube.

counts in the entire spectrum (within energy range 4–30 keV) amounted to 1371 counts/s (1092 counts/s in the continuous part of the spectrum). Assuming isotropic radiation distribution, this number is equivalent to  $2.7 \times 10^9$  photons/s in  $4\pi$  geometry (2.1 photons/s for continuous part of the spectrum). These values are less than those calculated from Equ. (3) for  $1 \mu\text{A}$  current; this discrepancy may be caused by neglecting the photons of energy less than 4 keV due to absorption in the air and in the detector entrance window. The experimentally measured ratio of number of counts in characteristic lines to number of counts in continuous part of the spectrum amounts to 0.255, and the mean photon energy is equal to 13.34 keV.

NAXT tube is almost a point-like source of X radiation emitted into  $4\pi$  geometry. Therefore, radiation dose rate strongly depends on the distance to the tube target. Measured dose rate vs. distance to tube target in the direction perpendicular and parallel to the tube axis is shown in Fig. 8. Measurements were taken by an air ionization chamber with a volume of  $0.2 \text{ cm}^3$ . The tube operating parameters were those used in brachytherapy:  $U_a = 30 \text{ kV}$ ,  $I_a = 20 \mu\text{A}$ . At these parameters the NAXT tube provides doses of the order of 1 Gy/min in the point 10 mm away from the tube target. Within distances closer to the tube target, dose spatial distribution would have to be measured with the help of a dosimeter with a higher spatial resolution.

## Thermal effects

At the values of accelerating voltages used in the NAXT tube, yield of the electron-photon conversion process is below 1% (Equ. (4)). In other words, 99% of the beam energy is converted into heat. In typical X-ray tubes this heat is dissipated to ambient by radiators or by forced cooling medium. Unfortunately, in case of the NAXT tube the heat must be transferred to the irradiated object, increasing its temperature.

Heat flow and hence the temperature distribution in the vicinity of the tube target depends on heat transport parameters of the object and on thermal coupling between the tube tip and surrounding layers of the object. In applications to brachytherapy, temperature of the surrounding human tissue should not rise more than by 4 K. This limits the admissible electron beam power to 0.8 W [3].

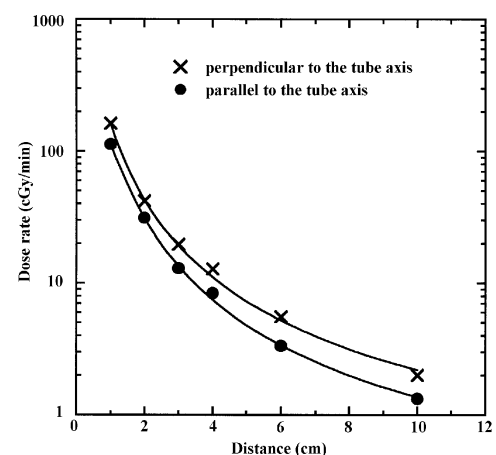
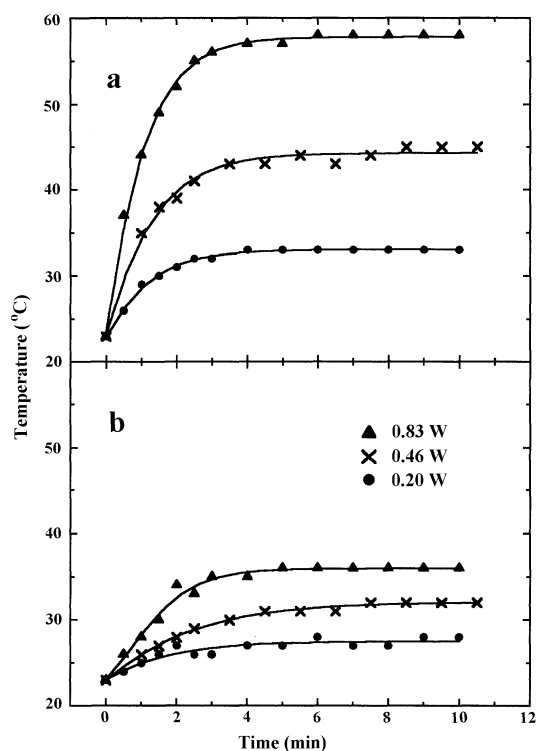


Fig. 8. Dose rate vs. distance to the tube target.



**Fig. 9.** Anode temperature in time after the tube has been switched on for three different power levels. Measurements taken on the anode surface 3 mm (a) and 40 mm (b) from the tip of the beryllium cap. Anode surrounded by air.

The rise of the tube anode temperature in time after the tube has been switched on is shown in Fig. 9. During these measurements the anode was surrounded by air. Temperature was measured on the anode surface 3 mm and 40 mm from the tip of the beryllium cap, for three power levels.

Results of similar measurements taken in water are shown in Fig. 10. Temperature was measured on the anode surface 3 mm from the tip of the beryllium cap, and in water in a point located 2 mm away from the anode surface.

## Conclusions

Preliminary tests confirm the NAXT tube developed in our Lab may be used in brachytherapy. Mean energy of the X-rays generated in the tube is several keV, and dose rates measured 10 mm away from the anode tip are of the order of 1 Gy/min. Such radiation source makes feasible performing brachytherapy in a single session lasting 20–30 minutes.

Electron beam target focal spot size may be regulated in the NAXT tubes. The tube may therefore be equally well applied in radiotherapy (beam diameter approximately 1.5 mm), and uniquely used to expose radiographs of selected fragments of body organs *in vivo* (beam diameter 0.2 mm).

In industrial applications like fluorescence analyzers or coating thickness gauges, the NAXT tube gives an opportunity to introduce its target close to the measured object, and

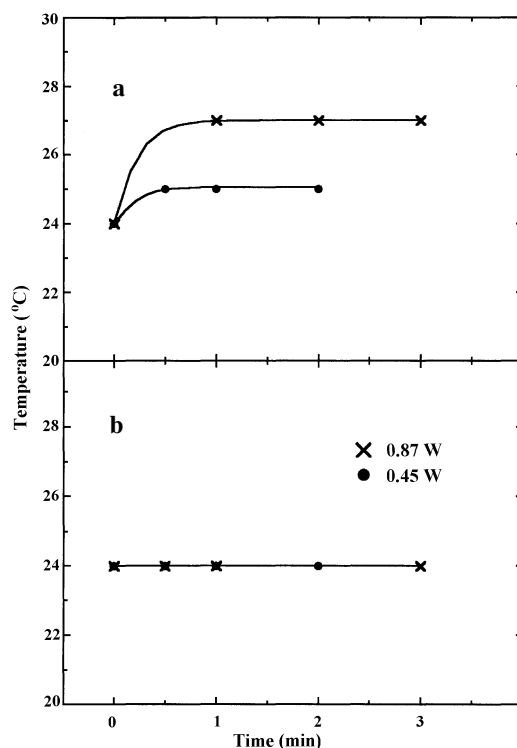


**Fig. 10.** Temperature in time measured for anode immersed in water: a – on the anode surface 3 mm from the tip of the beryllium cap; b – in water at a point located 2 mm away from the anode surface.

hence to avoid matrix effects related to interaction of X radiation with matter on its way from the target to the object. The tube may prove useful especially in measurements performed in liquid environments, where the target may be easily put in contact with the measured object, and the target-generated heat may be effectively dissipated.

Thanks to its beryllium cap design the NAXT tube is a point-like source of X-rays emitted into  $4\pi$  geometry. The design makes feasible fixing the solid angle into which the radiation is emitted.

It seems that the NAXT tube may prove especially useful in applications, in which cGy to kGy doses of X radiation must be deposited within small volumes.

## References

1. Dinsmore M, Harte KJ, Sliski AP *et al.* (1996) A new miniature X-ray source for interstitial radiosurgery: device description. *Med Phys* 23;1:45–52
2. Dyson NA (1973) X-rays in atomic and nuclear physics. Longman Group Limited, London
3. Hakim R, Zervas NT, Hakim F *et al.* (1997) Initial characterization of the dosimetry and radiobiology of a device for administering interstitial stereotactic radiosurgery. *Neurosurgery* 40;3:510–516
4. Skillicorn B (1982) X-ray tubes for energy dispersive XRF spectrometry. *Advance in X-Ray Analysis* 25:49–57
5. Yanch C, Zervas NT (1995) The photon radiosurgery system. *Sci Am Sci Med* 2;6:38–47